

KWEONHO KANG<sup>1\*</sup>, SEOK-MIN HONG<sup>1</sup>, CHANGHWA LEE<sup>1</sup>, YONGJUN CHO<sup>1</sup>THERMAL EXPANSION OF ZrO<sub>2</sub>-20 MOL% Gd<sub>2</sub>O<sub>3</sub>

The thermal expansion of a ZrO<sub>2</sub>-20 mol% Gd<sub>2</sub>O<sub>3</sub> pellet has been systematically investigated using a thermo-mechanical analyzer in the temperature range of 293-1773 K. Variations in the thermal expansion coefficient and density upon temperature change were calculated using the thermal expansion data. The average linear thermal expansion coefficient of the ZrO<sub>2</sub>-20 mol% Gd<sub>2</sub>O<sub>3</sub> pellet was found to be  $9.522 \times 10^{-6} \text{ K}^{-1}$  in the range of 298-1073 K. This value is smaller than that of ZrO<sub>2</sub> and larger than that of Gd<sub>2</sub>O<sub>3</sub>. Further, with an increase in temperature to 1773 K, the density of ZrO<sub>2</sub>-20 mol% Gd<sub>2</sub>O<sub>3</sub> pellet was found to decrease to 94.98 % of the initial density at 293 K.

*Keywords:* ZrO<sub>2</sub>-20 mol% Gd<sub>2</sub>O<sub>3</sub> pellet; thermal expansion; thermal expansion coefficient; density; thermo-mechanical analyzer

## 1. Introduction

Nuclear reactors require the use of higher contents of fissionable materials such as U-235 and Pu-249 to increase the maximum discharge burn-up and operation period. To this end, the use of Gd<sub>2</sub>O<sub>3</sub>, as a burnable poison is recommended owing to its ability to suppress the initial excess reactivity of the reactor core. It is used either in the form of a solid solution in the fuel matrix or in the form of a rod (Gd<sub>2</sub>O<sub>3</sub> or Gd<sub>2</sub>O<sub>3</sub>-ZrO<sub>2</sub>) in duplex type fuel. The duplex type fuel is considered superior to the solution type as it has the advantages of lower center-line temperature, easier fission gas release, and the absence of degradation of thermal conductivity attributed to the presence of the Gd-free fuel matrix. However, at elevated temperatures, compressive and tensile stresses and gap variation occur between the fuel and Gd<sub>2</sub>O<sub>3</sub> (or Gd<sub>2</sub>O<sub>3</sub>-ZrO<sub>2</sub>) rod as a result of the different degrees of thermal expansion of each material. Furthermore, the Gd<sub>2</sub>O<sub>3</sub>-ZrO<sub>2</sub> system has been widely used as an effective oxide ion conductor and is considered a promising candidate for the immobilization of plutonium for disposal. Owing to its significant merits, the Gd<sub>2</sub>O<sub>3</sub>-ZrO<sub>2</sub> system has become a subject of particular interest.

Kato et al. [1] developed the duplex type MOX-Gd<sub>2</sub>O<sub>3</sub> fuel for water reactors. The stability of Gd<sub>2</sub>O<sub>3</sub>-ZrO<sub>2</sub> system was investigated based on the melting point, X-ray diffraction (XRD) data, and thermogravimetric-differential thermal analy-

sis (TG-DTA) results. The Gd<sub>2</sub>Zr<sub>2</sub>O<sub>7</sub> phase of the pyrochlore structure was found to be stable below ~1500°C in the case of Gd<sub>0.5</sub>Zr<sub>0.5</sub>O<sub>y</sub> and the fluorite structure was stable up to the melting temperature in the case of Gd<sub>0.405</sub>Zr<sub>0.595</sub>O<sub>y</sub>. The melting temperatures of both the samples were over 2300°C. Kang et al. [2] investigated the in situ electrical conductivity of ZrO<sub>2</sub> stabilized with 10 mol% Gd<sub>2</sub>O<sub>3</sub> under gamma ray irradiation at an elevated temperature. Bhattacharyya and Agrawal [3] studied the phase, transformability, microstructure, and mechanical properties to investigate the effect of Gd<sub>2</sub>O<sub>3</sub> on the stabilization of ZrO<sub>2</sub>. Dutta et al. [4] studied the electrical and mechanical properties of ZrO<sub>2</sub>-Gd<sub>2</sub>O<sub>3</sub> ceramics with the Gd<sub>2</sub>O<sub>3</sub> concentration varying from 1.75 to 11 mol%. Wang et al. [5, 6] investigated the correlation of the crystal structures and structural properties of the fluorite- and pyrochlore-type compounds in the Gd<sub>2</sub>O<sub>3</sub>-ZrO<sub>2</sub> system by <sup>155</sup>Gd Mössbauer spectroscopy and powder X-ray diffraction. Rahaman et al. [7] studied the phase stability, sintering, and thermal conductivity of ZrO<sub>2</sub>-Gd<sub>2</sub>O<sub>3</sub> composites to investigate the feasibility of Gd<sub>2</sub>O<sub>3</sub> as an alternative stabilizer to Y<sub>2</sub>O<sub>3</sub> in ZrO<sub>2</sub>-based thermal barrier coating applications. Although a tremendous amount of effort has been devoted towards the study of the properties of the ZrO<sub>2</sub>-Gd<sub>2</sub>O<sub>3</sub> system, there is still a lack of data on its thermal expansion. Moreover, the thermal expansion influences the gap conductance between the fuel and ZrO<sub>2</sub>-Gd<sub>2</sub>O<sub>3</sub> rod as well as the thermal stress towards the fuel.

<sup>1</sup> KOREA ATOMIC ENERGY RESEARCH INSTITUTE, DAEJEON, REPUBLIC OF KOREA

\* Corresponding author: [nghkang@kaeri.re.kr](mailto:nghkang@kaeri.re.kr)



In this study, we investigated the thermal expansion of the  $\text{ZrO}_2$ -20 mol%  $\text{Gd}_2\text{O}_3$  rod using a TMA in the temperature range of 293-1773 K. In addition, the effect of temperature on thermal expansion coefficient and density was determined using the thermal expansion data.

## 2. Experimental

### 2.1. Materials

The thermal expansion of a sintered  $\text{ZrO}_2$ -20 mol%  $\text{Gd}_2\text{O}_3$  pellet was studied. The pellet was prepared based on the following procedure. Firstly,  $\text{ZrO}_2$  powder (99.8%, Alfa Aesar) and  $\text{Gd}_2\text{O}_3$  powder (99.9%, Alfa Aesar) were mixed for 1 h in a tubular mixer and milled for 2 h in a dynamic miller. To reduce the friction between the powders and between the powders and the die wall, 0.2 wt% zinc stearate was mixed with milled powder of  $\text{ZrO}_2$  and  $\text{Gd}_2\text{O}_3$  for 0.5 h. The mixed powder was then pressed under a pressure of  $300 \text{ MN m}^{-2}$  into green pellets. The pellets were sintered at 1973 K for 8 h under an argon flow at a heating and cooling rate of  $4 \text{ K min}^{-1}$ .

The XRD patterns of the sintered  $\text{ZrO}_2$ - $\text{Gd}_2\text{O}_3$  pellet are shown in Fig. 1, where the formation of the fluorite structure can be clearly observed.

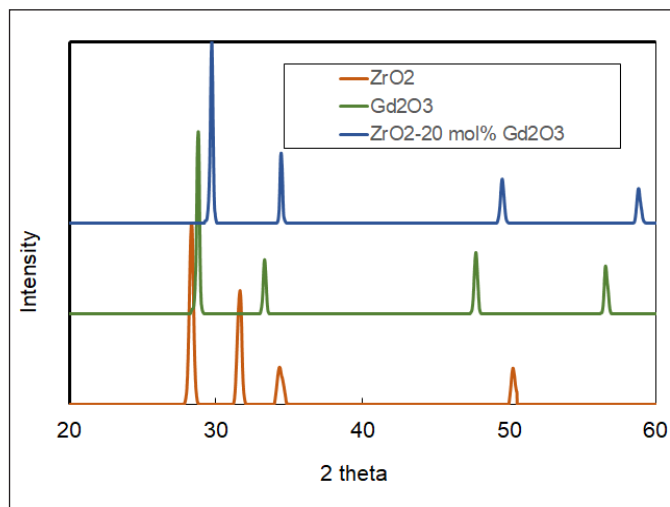


Fig. 1. XRD patterns of  $\text{ZrO}_2$ ,  $\text{Gd}_2\text{O}_3$  and  $\text{ZrO}_2$ -20 mol%  $\text{Gd}_2\text{O}_3$

The density of the sintered pellet was estimated to be  $6.24 \pm 0.02 \text{ g}\cdot\text{cm}^{-3}$  (98.15% of theoretical density), and the grain size was about 18.4 nm. The microstructure of the pellet was observed using scanning electron microscopy (SEM) is shown in Fig. 2.

### 2.2. Methods

The thermal expansion of the  $\text{ZrO}_2$ -20 mol%  $\text{Gd}_2\text{O}_3$  pellet was measured along the axial direction with a linear variable

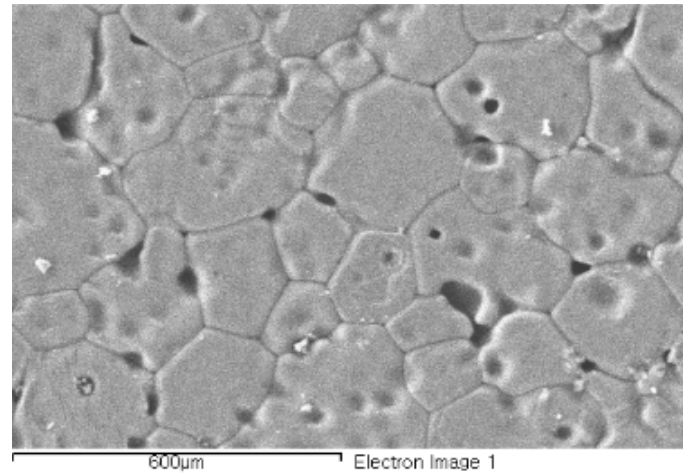


Fig. 2. The SEM image of  $\text{ZrO}_2$ -20 mol%  $\text{Gd}_2\text{O}_3$

differential transformer (LVDT) transducer in the temperature range of 293-1773 K using a push-rod-type TMA (Setaram). The measurements were performed at a constant heating rate of  $5 \text{ K min}^{-1}$  under an argon flow. The maximum error of the employed TMA was estimated to be within 2% for a standard material of  $\text{Al}_2\text{O}_3$ .

## 3. Results and discussion

Linear thermal expansion represents the ratio of the change in length to the initial length. It is calculated using the following expression [8]:

$$\text{Expansion, } \frac{\Delta L}{L_0}, \% = \frac{L_T - L_{293}}{L_{293}} \times 100 \quad (1)$$

where  $L_T$  and  $L_{293}$  represent the lengths of the specimens at temperatures  $T$  and 293 K, respectively. The linear thermal expansion value of the  $\text{ZrO}_2$ -20 mol%  $\text{Gd}_2\text{O}_3$  pellet measured in this study is plotted against temperature in Fig. 3. Open circles in Fig. 3 represent the experimental data while the red dashed line represents the fit.

The linear thermal expansion values of  $\text{Gd}_2\text{O}_3$  [8,9] and  $\text{ZrO}_2$  [10] are also shown in Fig. 3 for comparison. The linear thermal expansion value of the  $\text{ZrO}_2$ -20 mol%  $\text{Gd}_2\text{O}_3$  pellet was found to increase monotonically with increasing temperature. Moreover, the thermal expansion value of the  $\text{ZrO}_2$ -20 mol%  $\text{Gd}_2\text{O}_3$  pellet can be expressed as a function of temperature by using the following equation

$$\begin{aligned} \Delta L/L_0 (\%) = & -0.276 + 7.682 \times 10^{-4} T + \\ & + 1.604 \times 10^{-7} T^2 + 2.732 \times 10^{-11} T^3 \end{aligned} \quad (2)$$

where  $\Delta L$  represents the length variation with temperature and  $L_0$  represents the initial length at room temperature of 293 K.

In the fit obtained from this equation, the coefficient of determination  $R^2$  was 0.9999, implying high degree of match between experimental data and equation.

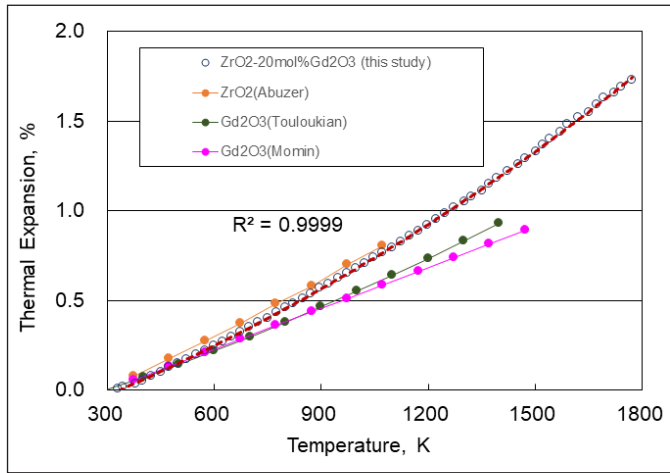


Fig. 3. Linear thermal expansion values of  $ZrO_2$ ,  $Gd_2O_3$ , and  $ZrO_2$ -20 mol%  $Gd_2O_3$  as a function of temperature

The corresponding instantaneous coefficient of the thermal expansion,  $\alpha$ , is defined by the following expression [8]:

$$\alpha = \frac{1}{L_{293}} \frac{dL}{dT} = \frac{1}{L_{293}} \frac{(L_2 - L_1)}{(T_2 - T_1)} \text{ at } T_m = \frac{T_2 + T_1}{2} \quad (3)$$

where  $L_{293}$ ,  $L_1$ , and  $L_2$  represent the lengths of the specimens at temperatures of 293 K,  $T_1$  and  $T_2$ , respectively. The instantaneous thermal expansion coefficient the  $ZrO_2$ -20 mol%  $Gd_2O_3$  pellet is plotted against temperature in Fig. 4. The instantaneous thermal expansion coefficients can be expressed as a function of temperature by using the following equation:

$$\alpha = 4.862 \times 10^{-3} T + 6.616 \quad (4)$$

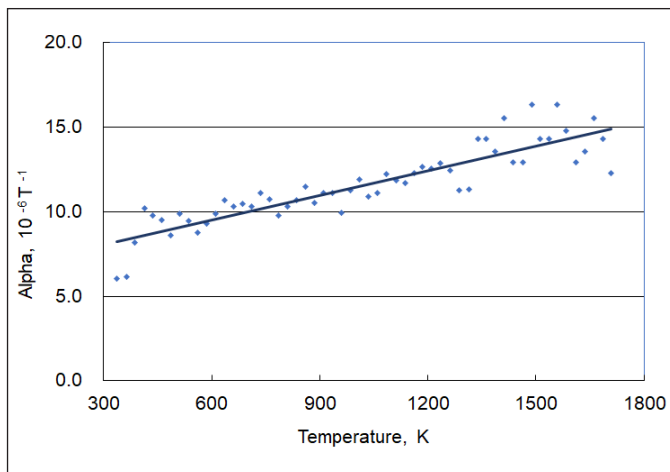


Fig. 4. Instantaneous thermal expansion coefficient of  $ZrO_2$ -20 mol%  $Gd_2O_3$  as a function of temperature

The average linear thermal expansion coefficient,  $\bar{\alpha}$ , is defined using the following equation:

$$\bar{\alpha} = \frac{1}{L_{293}} \frac{(L_T - L_{293})}{(T - 293)} \quad (5)$$

where  $L_{293}$  and  $L_T$  represent the lengths of the specimens at temperatures 293 K and  $T$ , respectively. The average linear thermal expansion coefficient of the  $ZrO_2$ -20 mol%  $Gd_2O_3$  pellet was found to be  $1.135 \times 10^{-5} K^{-1}$  in the temperature range of 298-1773 K. Further, when the temperature range was narrowed to 298-1073 K, the average linear thermal expansion coefficient of the  $ZrO_2$ -20 mol%  $Gd_2O_3$  pellet decreased to  $9.522 \times 10^{-6} K^{-1}$ . Since thermal expansion follows the second order of temperature, the average thermal expansion coefficient obtained in low temperature range is lower than that obtained in high temperature.

In the lower temperature range this value is lower than that of  $ZrO_2$  ( $10.0 \times 10^{-6}$  to  $10.4 \times 10^{-6} K^{-1}$  [10]), higher than that of  $Gd_2O_3$  ( $7.57 \times 10^{-6} K^{-1}$  [10]), and similar to the value calculated using the lever rule. A similar behavior was observed by Grover and Tyagi [11] in a  $CeO_2$ - $Gd_2O_3$  system, where they found that the incorporation of ceria, which has a relatively higher thermal expansion coefficient than gadolinia, into the lattice of gadolinia noticeably accelerated the thermal expansion of gadolinia.

Bentzen and Schwartzbach also found that the linear thermal expansion coefficient of the  $ZrO_2$ - $CeO_2$ - $Gd_2O_3$ - $Y_2O_3$  system increased with increasing temperature and Ce-content.

The density variations with temperature can be obtained from the thermal expansion data using the following equation [9]:

$$\rho(T) = \rho(298) \left( \frac{L_{298}}{L_T} \right)^3 \quad (6)$$

where  $\rho(T)$  and  $\rho(298)$  represent the densities of the specimens at temperature  $T$  and at 298 K, respectively. The relative density ( $\rho(T)/\rho(298)$ ) variations to the initial density of the  $ZrO_2$ -20 mol%  $Gd_2O_3$  pellet determined in this study are plotted against temperature in Fig. 5. Open circles in Fig. 5 represent the experimental data while the red dashed line represents the fit.

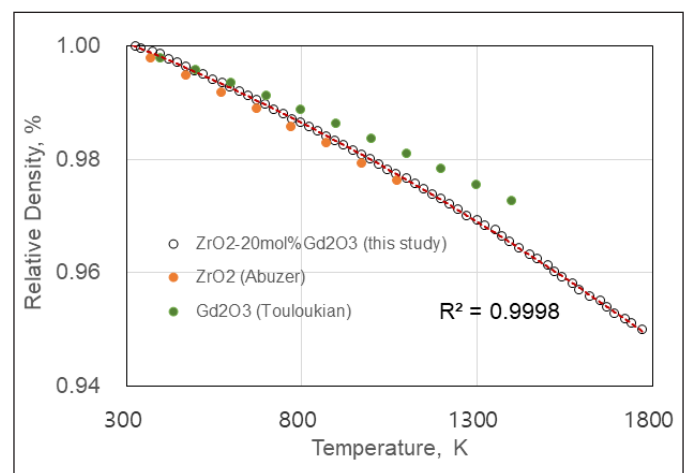


Fig. 5. Relative density of the  $ZrO_2$ -20 mol%  $Gd_2O_3$  pellet as a function of temperature

The relative density variation decreases monotonically with increasing temperature. As the temperature increased to 1773 K,

the relative density decreased to 94.98% of the initial density (at 298 K). The relative density variation of the ZrO<sub>2</sub>-20 mol% Gd<sub>2</sub>O<sub>3</sub> pellet can be expressed as a function of temperature using the following equation:

$$\rho(T)/\rho(293) = 1.008 - 2.125 \times 10^{-5} T + 6.507 \times 10^{-9} T^2 \quad (7)$$

where  $\rho(T)$  represents the density at a temperature of  $T$ , and  $\rho(298)$  represents the initial density at 298 K.

In the fit obtained from this equation, the coefficient of determination  $R^2$  was 0.9998, implying high degree of accordance between experimental data and equation.

#### 4. Conclusions

The thermal expansion of the ZrO<sub>2</sub>-20 mol.% Gd<sub>2</sub>O<sub>3</sub> pellet was measured using a TMA over the temperature range of 298-1773 K. The effect of temperature on the thermal expansion coefficient and density was also studied. Based on the obtained data, the following conclusions were drawn.

- (1) The thermal expansion coefficient of the ZrO<sub>2</sub>-20 mol.% Gd<sub>2</sub>O<sub>3</sub> pellet was found to be smaller than that of ZrO<sub>2</sub> and larger than that of Gd<sub>2</sub>O<sub>3</sub>.
- (2) In the temperature range of 298-1773 K, the average linear thermal expansion coefficient of the ZrO<sub>2</sub>-20 mol.% Gd<sub>2</sub>O<sub>3</sub> pellet was estimated to be  $1.135 \times 10^{-5} \text{ K}^{-1}$ .
- (3) The relative density of the ZrO<sub>2</sub>-20 mol.% Gd<sub>2</sub>O<sub>3</sub> pellet was found to decrease to 94.98% of the initial density at 298 K.

The data measured and calculated in the present study will be of considerable use for the performance evaluation of nuclear fuel.

#### Acknowledgment

This work was supported by a National Research Foundation of Korea (NRF) grant funded by the Korea Government (MSIT) (2021M2E3A1040059).

#### REFERENCES

- [1] M. Kato, S. Kohno, and K. Kamimura, Development of duplex type MOX-Gd<sub>2</sub>O<sub>3</sub> for water reactor, in: Technical Committee Meeting on Advances in Pellet Technology for Improved performance at High Burnup, Tokyo, Japan (1996).
- [2] K. Thae-Khapp, K. Il-Hiun, Y. Katano, N. Igawa, H. Ohno, *J. Nucl. Mater.* **209**, 321 (1994). DOI: [https://doi.org/10.1016/0022-3115\(94\)90270-4](https://doi.org/10.1016/0022-3115(94)90270-4)
- [3] S. Bhattacharyya, D.C. Agrawal, *J. Mater. Sci.* **37**, 1387 (2002). DOI: <https://doi.org/10.1023/A:1014572629824>
- [4] S. Dutta, S. Bhattacharya, D.C. Agrawal, *Mater. Sci. Eng. B* **100**, 191 (2003). DOI: [https://doi.org/10.1016/S0921-5107\(03\)00105-3](https://doi.org/10.1016/S0921-5107(03)00105-3)
- [5] J. Wang, A. Nakamura, M. Takeda, *Solid State Ionics* **164**, 185 (2003). DOI: <https://doi.org/10.1016/j.ssi.2003.09.003>
- [6] J. Wang, H. Otake, A. Nakamura, M. Takeda, *J. Solid State Chem.* **176**, 105 (2003). DOI: [https://doi.org/10.1016/S0022-4596\(03\)00353-0](https://doi.org/10.1016/S0022-4596(03)00353-0)
- [7] M.N. Rahaman, J.R. Gross, R.E. Dutton, H. Wang, *Acta Mater.* **554**, 1615 (2006).
- [8] Y.S. Touloukian, *Thermophysical Properties of Matter*, vol. 12, IFI/Plenum, New York (1970).
- [9] A.C. Momin, M.D. Mathews, *Indian J. Chem.* **15a**, 1096 (1977).
- [10] A. Özsunar, *Materials and Design* **29**, 1690 (2008). DOI: <https://doi.org/10.1016/j.matdes.2008.03.029>
- [11] V. Grover, A.K. Tyagi, *Mater. Res. Bull.* **39**, 859 (2004). DOI: <https://doi.org/10.1016/j.materresbull.2004.01.007>
- [12] J.J. Bentzen, H. Schwartzbach, *Solid State Ionics* **40-41**, 942 (1990). DOI: [https://doi.org/10.1016/0167-2738\(90\)90159-O](https://doi.org/10.1016/0167-2738(90)90159-O)